Available online at www.sciencedirect.com
ScienceDirect
Journal of Organometallic Chemistry 692 (2007) 5103–5108
Journal of Organometallic Chemistry
www.elsevier.com/locate/jorganchem

Note

Electronic structures of organometallic complexes of f elements LXVI [☆] Parametric analysis of the linear dichroism spectrum of an oriented tris(η^5-tetramethylcyclopentadienyl)samarium(III) single crystal

Hanns-Dieter Amberger [*], Hauke Reddmann

Institut für Anorganische und Angewandte Chemie der, Universität Hamburg, Martin-Luther-King-Platz 6, 20146 Hamburg, Germany

Received 19 April 2007; received in revised form 4 July 2007; accepted 20 July 2007
Available online 27 July 2007

Abstract

The absorption spectra of pseudo (ψ) trigonal planar Sm(η^5-$C_5Me_4H)_3$ (**1**) and La(η^5-$C_5Me_4H)_3$ (**2**) in KBr pellets have been measured at room temperature and 77 K, respectively. Additionally, the linear dichroism spectra of σ and π type of an oriented single crystal of **1** have been recorded at ambient temperature. The observed polarization properties of the f–f transitions allowed the assignment of the transitions. The free parameters of a phenomenological Hamiltonian were fitted to the energies of the assigned terminal levels, leading to a reduced r.m.s. deviation of 19.1 cm^{-1} for 19 assignments. On the basis of these phenomenological CF parameters, the global CF strength experienced by the Sm^{3+} central ion was estimated, and seems to be the largest one ever encountered in samarium(III) chemistry. The obtained Slater parameter F^2 and the spin–orbit coupling parameter ζ_{4f} allow the insertion of compound **1** into empirical nephelauxetic and relativistic nephelauxetic series, respectively. On the basis of these models, complex **1** turns out to be the most covalent Sm^{III} compound found to date. The experimentally-based non-relativistic molecular orbital scheme (in the f range) of complex **1** was determined and compared with the results of a previous Xα-SW calculation on the ψ trigonal planar model compound Sm(η^5-$C_5H_5)_3$.

Keywords: Samarium; Substituted cyclopentadienyl ligand; Linear dichroism spectrum; Crystal field analysis; Molecular orbital scheme

1. Introduction

$LnCp'_3$ complexes with sterically demanding Cp′ ligands such as C_5H_4Z or $C_5H_3Z_2$ (where Z corresponds to a bulky substituent) and C_5Me_4R (R = H, Me, Et, *i*Pr, $SiMe_3$) have pseudo (ψ) trigonal planar molecular structures [2–4]. The most popular series among the above-mentioned $LnCp'_3$ compounds are the $Ln(C_5Me_5)_3$ complexes (Ln = La, Ce, Pr, Nd, Sm, Gd, Y) [3–5], frequently denoted by $LnCp^*_3$. Although a rich chemistry has been developed with $LnCp^*_3$ compounds [3–5], almost nothing is known about the spectrochemical, nephelauxetic and relativistic nephelauxetic effects associated with the Cp^* ligand.

In recent years, the low temperature absorption spectra of the pair of compounds $Nd(C_5Me_4H)_3$/$NdCp^*_3$ were simultaneously recorded at Hamburg (KBr pellet, He bath cryostat [6,7]) and Wroclaw (Halowax mull, He transfer cryostat [6,8]). Whereas the absorption spectra of $Nd(C_5Me_4H)_3$ were identical within experimental error, those of $NdCp^*_3$ differed not only from each other, but also from that of $Nd(C_5Me_4H)_3$ [6–8]. In spite of these disappointing findings, the same procedure was recently repeated (at Hamburg) with the pair $Sm(C_5Me_4H)_3$/$SmCp^*_3$. Now, however, the absorption spectra of both compounds were not only independent of the matrix (KBr, CsI) but also of temperature (vide infra), thus indicating an energetically isolated crystal field (CF) ground state. Also, the spectra of both compounds are similar, which suggests that both complexes have comparable CF splitting patterns. This finding offers the unique chance to understand the electronic structure

[☆] For part LXV, see [1].

[*] Corresponding author. Tel.: +49 40 42838 3524; fax: +49 40 42838 2893.
E-mail address: fc3a501@uni-hamburg.de (H.-D. Amberger).

0022-328X/$ - see front matter © 2007 Elsevier B.V. All rights reserved.
doi:10.1016/j.jorganchem.2007.07.028

of $SmCp^*_3$, provided that the CF splitting pattern of $Sm(C_5Me_4H)_3$ (**1**) is known.

In the case of air-stable compounds, cut- and polishable single crystals allow the symmetries of the CF levels of the Ln compound under consideration to be derived from the optical spectra of α, σ and π oriented single crystals with respect to the propagation direction and polarization of the electromagnetic radiation to be absorbed or scattered (linear dichroism spectra, LD) [9, p. 158], [10, p. 98]. Organometallic Ln complexes are usually air-sensitive, have poor crystallizing properties, are prone to phase transitions, and additionally the principal rotation axes of the individual molecules in the unit cell are frequently not aligned [1]. Even if they were aligned, as in the case of low-symmetric crystal systems, it is difficult to orientate these rotation axes with respect to an external vector field [1]. Thus, during the latest decades the results of LD measurements of f element organyls were only reported for the σ complexes $Ln\{CH(SiMe_3)_2\}_3$ (Ln = Nd, Er [1]), and some base adducts of the $LnCp_3$ moiety (Ln = Pr, Nd [1]). Recent efforts to apply this method also to homoleptic $LnCp'_3$ complexes temporarily failed for $LnCp^*_3$ (Ln = Nd, Sm) [7], but were successful for $Nd(C_5Me_4H)_3$ [1].

In the present paper, the (assigned) CF splitting pattern of complex **1** is derived on the basis of optical polarization measurements. Subsequently, this experimental CF splitting pattern will be simulated by fitting the free parameters of a phenomenological Hamiltonian [9, p. 167]. From the parameters found, the $[C_5Me_4H]^-$ ligand can be inserted into empiric spectrochemical, nephelauxetic and relativistic nephelauxetic series of Sm^{III} compounds. Also, the experimentally-based non-relativistic molecular orbital (MO) scheme (in the f range) [11] of **1** can be set up, and will be compared with the results of a previous Xα-SW calculation on the ψ trigonal planar model complex $Sm(\eta^5\text{-}C_5H_5)_3$ [12].

Utilizing the present results, we will perform a parametric analysis of the absorption spectrum of $SmCp^*_3$ in a subsequent paper.

2. Experimental

$Sm(C_5Me_4H)_3$ and $La(C_5Me_4H)_3$ (**2**) were purchased from Sigma–Aldrich. Single crystals were grown by slowly cooling down nearly saturated solutions of **1** in toluene from ca. 80 °C to room temperature. The absorption and LD spectra were recorded by means of a Cary 5E instrument and polarizer foils (model 27360, Oriel).

3. Results and discussion

According to an X-ray diffraction study, compound **1** crystallizes in the space group $R\bar{3}$ (No. 148) with two ψ trigonal planar molecules in the unit cell [13]. The threefold axes of these molecules are not only parallel to each other, but also to the main axis of the rod-like single crystal. Thus, for **1** the orientation problem of the threefold molecular axes with respect to the propagation and polarization directions of the beam to be absorbed or scattered is minimized.

The ψ trigonal planar molecular geometry of complex **1** corresponds to a CF of D_{3h} symmetry. The free Sm^{3+} ion gives rise to multiplets $^{2S+1}L_J$ with $1/2 \leqslant J \leqslant 15/2$ (in the range up to 12000 cm^{-1}), which are split by the CF into Kramers doublets of Γ_7, Γ_8 and Γ_9 symmetry, respectively (double group D'_{3h}).

In the case of yellow or orange organometallic Sm^{III} compounds the CF splitting patterns of the low-lying multiplets ^6H_J can be derived from the luminescence spectrum originating from $^4G_{5/2}$ [14]. The $^4G_{5/2}$ multiplet of the dark brown red complex **1**, however, does not fluoresce, thus only the absorption spectrum (starting at ca. 4000 cm^{-1}) can give information about the CF splitting pattern. Unfortunately, not only C–H combination vibrations and overtones interfere with f–f signals in the lower range (4000–6000 cm^{-1}), but also a strong charge transfer band (which starts at ca. 15000 cm^{-1}) obscures the CF splitting of $^4G_{5/2}$ and higher multiplets and is the reason no fluorescence is observed. Thus only a very limited number of f–f transitions are experimentally accessible.

Model calculations using the electrostatic point charge model [9, p. 189], the angular overlap model [15,16], the Xα-SW approximation [17] and the results of a parametric analysis of the absorption spectrum of $Sm(C_5H_4tBu)_3$ [18] suggest that for **1** an energetically isolated CF level of Γ_7 symmetry is the ground state [7,12,18]. In this case, according to the selection rules of D_{3h} symmetry [9, p. 255], transitions to Γ_7 levels are forbidden. In the π spectrum, only transitions to terminal Γ_8 level are allowed, and in the σ spectrum both Γ_8 and Γ_9 levels give rise to signals (the latter also holding for solutions or pellets). Thus, signals in the π spectrum can be assigned to excited Γ_8 levels, and additional bands in the σ or pellet spectrum (with respect to the π spectrum) to terminal levels of Γ_9 symmetry.

All single crystals of **1** at our disposal were somewhat too thick, thus only the π spectrum could be recorded completely in the f–f-range, whereas the absorbance of a number of strong absorption peaks (in the range 5000–9000 cm^{-1}) was too high for recording a complete σ spectrum. According to the above separation scheme, however, the difficult growth of an optically diluted single crystal was unnecessary.

At 77 K, a KBr pellet of **1** shows a number of sharp absorption signals in the range 4000–5300 cm^{-1} which might correspond partly to f–f transitions. However, with the exception of the signals at 4449, 4755 and 5129 cm^{-1}, most of them appear also in the absorption spectrum of a KBr pellet of compound **2**, suggesting that they are due to C–H combination vibrations or overtones. The polarization properties of the signals in this energy range of presumably f–f origin cannot be observed clearly, thus no assignments are possible at the present stage and the spectra are not shown.

For reasons of clarity, the remaining part of the absorption spectrum (the 77 K spectrum of a KBr pellet is preferred to the room temperature spectrum, as the f–f transitions are much sharper here and stronger than the C–H combination vibrations, however shifted up to 25 cm^{-1} to higher energies) is divided into three sections (see Figs. 1–3). Applying the above-mentioned identification scheme, a number of levels of Γ_8 and Γ_9 symmetry, respectively, could be assigned (see Figs. 1–3, Table 1).

The free parameters of a phenomenological Hamiltonian [9, p. 167], were fitted to the assigned levels. As the starting parameter set for the free ion and the CF parameters B_q^k, those of $Sm(C_5H_4tBu)_3$ [18] and $Nd(C_5Me_4H)_3$ [1] were chosen, respectively. After some fitting cycles (only the Slater, spin–orbit coupling and the CF parameters were varied), a reduced r.m.s. deviation [9, p. 164], of 19.1 cm^{-1} was achieved for 19 assignments (see Tables 1 and 2). The assigned CF states with energies higher than 9600 cm^{-1} were not considered in this calculation because of strong deviations between calculated and experimental values, presumably due to the adjacent charge-transfer band.

The parameter $N_v/\sqrt{4\pi} = \sum_{k,q}\sqrt{\frac{(B_q^k)^2}{2k+1}}$ is considered as a relative measure of the CF strength experienced by the central Ln^{3+} ion [20]. Inserting the CF parameters of **1** into the above-mentioned relation, one ends up with an $N_v/\sqrt{4\pi}$ value of 1813 cm^{-1}. In Table 3, this value is compared with those of other Sm^{III} compounds. Obviously, the central ion of complex **1** experiences the highest CF strength found to date for Sm^{III} compounds. That of homoleptic $Sm(C_5H_4t$-$Bu)_3$ is only somewhat, but those of mono and, especially, bis base adducts ($[La_{0.8}Sm_{0.2}(Cp)_3(NCCH_3)_2]$ [14] or $Sm(C_5H_4CH_2CH_2OCH_3)_3$ [21]) are considerably lower

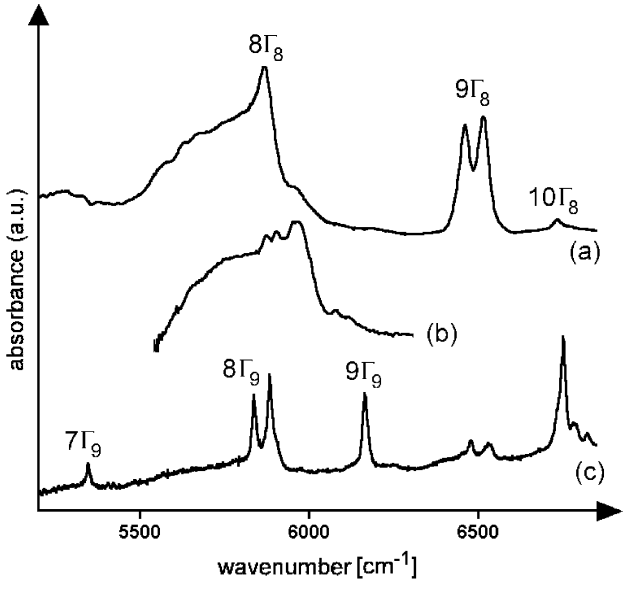

Fig. 1. Absorption spectra of $Ln(C_5Me_4H)_3$: (a) Ln = Sm, π spectrum, in the range 5300–7000 cm^{-1}, room temperature; (b) Ln = La, KBr pellet, in the range 5550–6300 cm^{-1}, room temperature; (c) Ln = Sm, KBr pellet, in the range 5300–7000 cm^{-1}, 77 K.

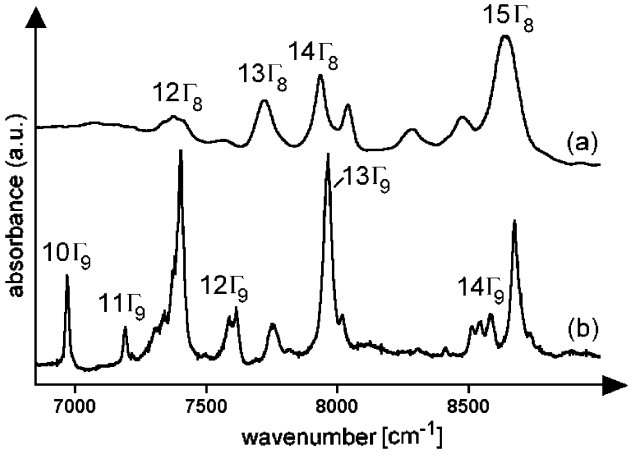

Fig. 2. Absorption spectrum of $Sm(C_5Me_4H)_3$ in the range 6900–9000 cm^{-1}: (a) π spectrum, room temperature; (b) KBr pellet, 77 K.

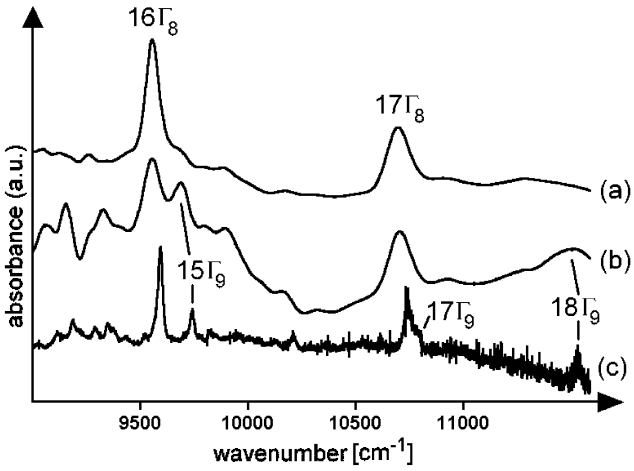

Fig. 3. Absorption spectrum of $Sm(C_5Me_4H)_3$ in the range 9000–11700 cm^{-1}: (a) π spectrum, room temperature; (b) σ spectrum, room temperature; (c) KBr pellet, 77 K.

(see Table 3). This finding may be explained by the longer Ln–C distances of the bis and mono adducts compared to the base free complexes [22]. Furthermore, according to the results of model calculations, the addition of one and, even more, of two axial ligands considerably reduces (assuming constant Ln–C bond lengths) the absolute value of the dominant CF parameter B_0^2, leading to lower $N_v/\sqrt{4\pi}$ values [11]. These explanations are consistent with the considerably smaller total splitting of f orbitals in the experimentally-based MO schemes of $[La_{0.8}Sm_{0.2}(Cp)_3$-$(NCCH_3)_2]$ and $[Sm(C_5H_4tBu)_3(THF)]$ as compared to $Sm(C_5H_4tBu)_3$ [18].

The Slater parameter F^2 and the spin–orbit coupling parameter of the gaseous Sm^{3+} ion are unknown, thus the nephelauxetic parameter $\beta = F^2(\text{complex})/F^2(\text{free ion})$, the relativistic nephelauxetic parameter $\beta' = \zeta_{4f}(\text{complex})/\zeta_{4f}(\text{free ion})$, and the covalency $\sqrt{b}$ (defined as $\sqrt{b} = \sqrt{(1-\beta)/2}$ [23]) cannot be calculated. The insertion of compound **1** into truncated empiric nephelauxetic and

Table 1
Calculated and experimental energy levels (at 77 K) for $Sm(C_5Me_4H)_3$

Multiplet	CF level		E (calc.)	E (exp.)
$^6H_{5/2}$[a]	$1\Gamma_7$[b]	$\pm5/2$[c]	0	0
$^6H_{5/2}$	$1\Gamma_9$	$\pm3/2$	556	
$^6H_{7/2}$	$2\Gamma_7$	$\pm7/2$	914	
$^6H_{5/2}$	$1\Gamma_8$	$\pm1/2$	1034	
$^6H_{7/2}$	$3\Gamma_7$	$\pm5/2$	1649	
$^6H_{7/2}$	$2\Gamma_9$	$\pm3/2$	1911	
$^6H_{7/2}$	$2\Gamma_8$	$\pm1/2$	2006	
$^6H_{9/2}$	$3\Gamma_9$	$\pm9/2$	2546	
$^6H_{9/2}$	$4\Gamma_7$	$\pm7/2$	2750	
$^6H_{9/2}$	$3\Gamma_8$	$\pm1/2$	3034	
$^6H_{9/2}$	$4\Gamma_9$	$\pm3/2$	3127	
$^6H_{9/2}$	$5\Gamma_7$	$\pm5/2$	3147	
$^6H_{11/2}$	$4\Gamma_8$	$\pm11/2$	3607	
$^6H_{11/2}$	$5\Gamma_9$	$\pm9/2$	3878	
$^6H_{11/2}$	$6\Gamma_7$	$\pm7/2$	4196	
$^6H_{11/2}$	$5\Gamma_8$	$\pm1/2$	4450	4449
$^6H_{11/2}$	$6\Gamma_9$	$\pm3/2$	4515	
$^6H_{11/2}$	$7\Gamma_7$	$\pm5/2$	4603	
$^6H_{13/2}$	$6\Gamma_8$	$\pm13/2$	4753	4755
$^6H_{13/2}$	$7\Gamma_8$	$\pm11/2$	5093	
$^6H_{13/2}$	$7\Gamma_9$	$\pm9/2$	5326	5344
$^6H_{13/2}$	$8\Gamma_7$	$\pm7/2$	5409	
$^6H_{15/2}$	$8\Gamma_9$	$\pm15/2$	5835	5836
$^6H_{13/2}$	$8\Gamma_8$	$\pm1/2$	5893	5883
$^6H_{13/2}$	$9\Gamma_7$	$\pm5/2$	6121	
$^6H_{13/2}$	$9\Gamma_9$	$\pm3/2$	6180	6164
$^6H_{15/2}$	$9\Gamma_8$	$\pm13/2$	6497	6478
$^6H_{15/2}$	$10\Gamma_8$	$\pm11/2$	6757	6749
$^6H_{15/2}$	$10\Gamma_9$	$\pm9/2$	6957	6970
$^6F_{1/2}$	$11\Gamma_8$	$\pm1/2$	7011	
$^6H_{15/2}$	$10\Gamma_7$	$\pm7/2$	7195	
$^6F_{3/2}$	$11\Gamma_9$	$\pm3/2$	7238	7192
$^6F_{3/2}$	$12\Gamma_8$	$\pm1/2$	7405	7401
$^6H_{15/2}$	$11\Gamma_7$	$\pm5/2$	7527	
$^6H_{15/2}$	$12\Gamma_9$	$\pm3/2$	7608	7606
$^6F_{5/2}$	$12\Gamma_7$	$\pm5/2$	7706	
$^6H_{15/2}$	$13\Gamma_8$	$\pm1/2$	7741	7749
$^6F_{5/2}$	$14\Gamma_8$	$\pm1/2$	7941	7957
$^6F_{5/2}$	$13\Gamma_9$	$\pm3/2$	7950	7957
$^6F_{7/2}$	$13\Gamma_7$	$\pm7/2$	8512	
$^6F_{7/2}$	$14\Gamma_9$	$\pm3/2$	8591	8583
$^6F_{7/2}$	$15\Gamma_8$	$\pm1/2$	8643	8671
$^6F_{7/2}$	$14\Gamma_7$	$\pm5/2$	8659	
$^6F_{9/2}$	$16\Gamma_8$	$\pm1/2$	9583	9593
$^6F_{9/2}$	$15\Gamma_9$	$\pm3/2$	9648	(9726)
$^6F_{9/2}$	$15\Gamma_7$	$\pm5/2$	9649	
$^6F_{9/2}$	$16\Gamma_7$	$\pm7/2$	9819	
$^6F_{9/2}$	$16\Gamma_9$	$\pm9/2$	9822	(9819)
$^6F_{11/2}$	$17\Gamma_8$	$\pm1/2$	10842	(10731)
$^6F_{11/2}$	$17\Gamma_9$	$\pm3/2$	10852	(10777)
$^6F_{11/2}$	$17\Gamma_7$	$\pm5/2$	10894	
$^6F_{11/2}$	$18\Gamma_7$	$\pm7/2$	11009	
$^6F_{11/2}$	$18\Gamma_9$	$\pm9/2$	11184	(11170)
$^6F_{11/2}$	$18\Gamma_8$	$\pm11/2$	11410	(11529)

All values in cm^{-1}.
[a] Dominating Russell–Saunders multiplet $^{2S+1}L_J$.
[b] The Bethe Γ notation for the double group D'_{3h} is used. The irreps Γ_i are ordered in ascending energy.
[c] Largest eigenvector component $\pm M_J$.
[d] Energies in parentheses were not used in the fit.

relativistic nephelauxetic series can be seen from Table 3. Evidently, the truncated nephelauxetic series for Sm^{III} compounds in Table 3 is only partly followed by the trend

Table 2
Parameter values for $Sm(C_5Me_4H)_3$, $Sm(C_5H_4tBu)_3$ and $Nd(C_5Me_4H)_3$

Parameter	$Sm(C_5Me_4H)_3$	$Sm(C_5H_4tBu)_3$[a]	$Nd(C_5Me_4H)_3$[b]
F^2	72824	73992	69800
F^4	57547	58470	51172
F^6	36801	37391	35380
ζ_{4f}	1130	1143	878
α	[21.6][c]	[21.6]	[21.35]
β	[−724]	[−724]	[−680.22]
γ	[1700]	[1700]	[1586]
T^2	[291]	[291]	[377]
T^3	[13]	[13]	[40]
T^4	[34]	[34]	[63]
T^6	[−193]	[−193]	[−292]
T^7	[288]	[288]	[358]
T^8	[330]	[330]	[354]
M^0	[2.4]	[2.4]	[1.97]
M^2	[1.34]	[1.34]	[1.1]
M^4	[0.91]	[0.91]	[0.75]
P^2	[341]	[341]	[255]
P^4	[256]	[256]	[191]
P^6	[171]	[171]	[127]
B_0^2	−2971	−2809	−3037
B_0^4	1304	1483	1028
B_0^6	1433	1278	1096
B_6^6	−2765	−2685	−2307
$N_v/\sqrt{4\pi}$	1813	1749	1695
σ	19.1 (19)[d]	17.5 (25)	16.1 (38)

All values in cm^{-1}.
[a] From Ref. [18].
[b] From Ref. [1].
[c] Values in brackets held fixed on the values of $LaCl_3:Sm^{3+}$ [19] or $LaCl_3:Nd^{3+}$ [19], resp.
[d] Number of fitted energies in parentheses.

Table 3
Comparison of the F^2, ζ_{4f} and $N_v/\sqrt{4\pi}$ values of $Sm(C_5Me_4H)_3$ with those of selected Sm^{III} compounds (from Ref. [18])

Compound[a]	F^2	ζ_{4f}	$N_v/\sqrt{4\pi}$
$LaF_3:Sm^{3+}$	79805	1176	610
$[Na_3\{Sm(ODA)_3\}\bullet2NaClO_4\bullet6H_2O]$[b]	79015	1166	755
$Sm(Cp)(Tp^{Me}2)_2$	78293	1159	522
$GdOCl:Sm^{3+}$	78196	1150	640
$LaCl_3:Sm^{3+}$	78125	1168	300
$Cs_2NaSmCl_6$	77510	1167	545
$[La_{0.8}Sm_{0.2}(Cp)_3(NCCH_3)_2]$	77002	1155	1222
$[Sm\{N(SiMe_3)_2\}_3(CNC_6H_{11})_2]$	76676	1169	891
$Sm(C_5H_4CH_2CH_2OCH_3)_3$	76602	1156	1198
$Sm\{N(SiMe_3)_2\}_3$	76388	1164	1179
$[Sm(C_5H_4SiEt_3)_3(NCCH_3)]$	76305	1149	1375
$[Sm(Cp)_3(NCCH_3)]$	76230	1148	1324
$[Sm(Cp)_3(CNC_6H_{11})]$	75813	1151	1373
$[Sm(Cp)_3(THF)]$	75773	1149	1378
$[Sm(C_5H_4tBu)_3(THF)]$	75324	1149	1371
$Sm(C_5H_4tBu)_3$	73992	1143	1749
$Sm(C_5Me_4H)_3$	72824	1130	813

All values in cm^{-1}.
[a] Ordered by decreasing Slater parameter F^2.
[b] ODA = oxydiacetato.

of ζ_{4f} values, and thus the relativistic nephelauxetic series. Obviously, complex **1** has the lowest F^2 value and thus is the most covalent Sm^{III} compound (considering only f orbitals) hitherto analyzed.

As expected, the close-lying 15 C atoms of the three $[C_5Me_4H]^-$ ligands produce stronger nephelauxetic effects than the more distant C atoms of mono and bis adducts. Besides, the C atoms of **1** at an average distance of 276 pm [13] give rise to a stronger nephelauxetic effect than the N atoms of the three $[N(SiMe_3)_2]^-$ ligands of $Sm\{N(SiMe_3)_2\}_3$ at an average distance of 228.4 pm [24].

The eigenvalues of an energy matrix of the spin-free f^1 system, into which the CF parameters of a previous parametric analysis of the compound of interest had been inserted, were defined in Ref. [11] as the experimentally-based non-relativistic MO scheme of this compound in the f range.

In Fig. 4, the experimentally-based non-relativistic MO scheme (in the f range) of complex **1** is compared with the non-relativistic MO scheme of the ψ trigonal planar model complex $Sm(\eta^5\text{-}C_5H_5)_3$ calculated in the framework of the Xα-SW approximation [12]. Obviously, the calculated total splitting of f orbitals is considerably greater than the experimentally-based one.

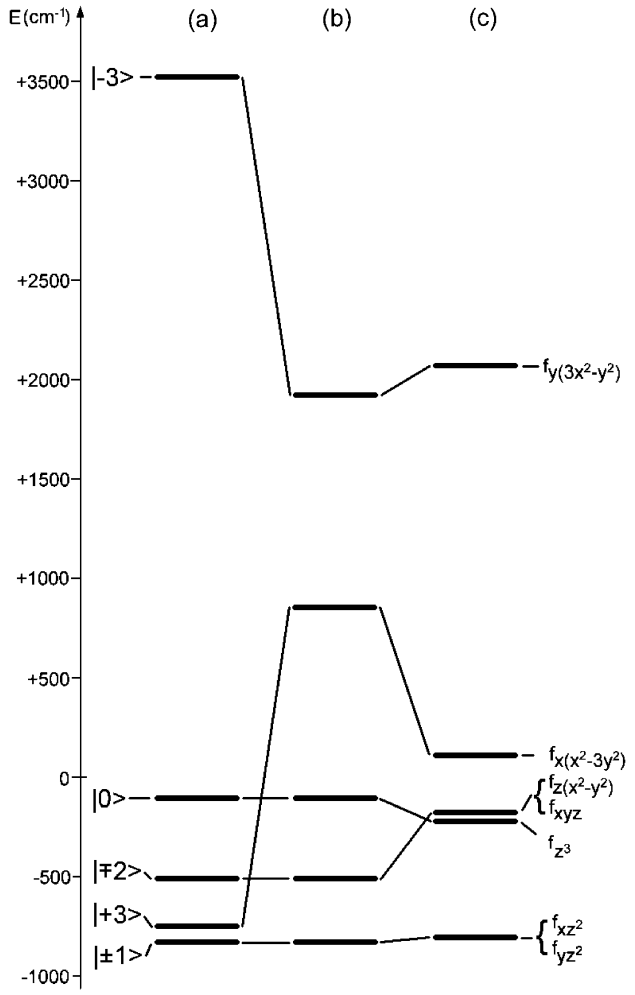

Fig. 4. Experimentally-based and calculated non-relativistic MO schemes of: (a) ψ trigonal planar $Sm(\eta^5\text{-}Cp)_3$ (calc., from Ref. [12]); (b) dito, but B_6^6 reduced to a quarter; (c) $Sm(C_5Me_4H)_3$, experimentally-based.

Fitting the free parameters of the phenomenological Hamiltonian of the spin-free f^1 system to the calculated energies of f orbitals of $Sm(\eta^5\text{-}C_5H_5)_3$ one arrives at $B_0^2 = -3443\ cm^{-1}$, $B_0^4 = 2817\ cm^{-1}$, $B_0^6 = 1296\ cm^{-1}$ and $B_6^6 = -6033\ cm^{-1}$ [18]. Comparing these values with those of compound **1** (see Table 2), it becomes evident that first of all the CF parameters B_6^6 (which considers the interactions between orbitals $f_{x(x^2-3y^2)}$ and $f_{y(3x^2-y^2)}$ within the framework of CF theory) but also B_0^4 are heavily overestimated by the model calculation. To roughly reproduce the correct total splitting of f orbitals, B_6^6 has to be reduced to a quarter, giving also a nearly correct sequence of levels (the closely-lying states $|0\rangle$ and $|\mp 2\rangle$ are interchanged, see Fig. 4).

4. Conclusions

Compound **1** represents the second homoleptic π complex of f elements for which LD measurements have been performed successfully. The fit of the (assigned) CF energies leads to free ion and crystal field parameters, the interpretation of which demonstrates that **1** is the most covalent Sm^{III} compound known to date (considering only the f electrons) and that the Sm^{3+} central ion of **1** experiences the largest CF strength ever encountered in samarium(III) chemistry.

A non-relativistic model calculation (Xα-SW approximation) on the ψ trigonal planar $Sm(\eta^5\text{-}Cp)_3$ overestimates the total splitting of f orbitals by a factor of 1.5 (compared with the experimentally-based non-relativistic one).

Because of the similarity of the absorption spectra of complex **1** and $SmCp^*_3$ and the electronic structure of **1** having been solved here, there exists a good chance for a future successful parametric analysis of the absorption spectrum of the latter compound, thus permitting the Cp^* ligand to be inserted into the spectrochemical, nephelauxetic and relativistic nephelauxetic series, at least for Sm^{III} compounds.

Acknowledgement

The financial support of the "Deutsche Forschungsgemeinschaft" is gratefully acknowledged.

References

[1] H.-D. Amberger, H. Reddmann, Z. Anorg. Allg. Chem. 633 (2007) 443–452, and references therein.
[2] H. Schumann, J.A. Meese-Marktscheffel, L. Esser, Chem. Rev. 95 (1995) 865–986, and references therein.
[3] W.J. Evans, B.L. Davis, Chem. Rev. 102 (2002) 2119–2136, and references therein.
[4] W.J. Evans, J.M. Perotti, S.A. Kozimor, T.M. Champagne, B.L. Davis, G.W. Nyce, C.H. Fujimoto, R.D. Clark, M.A. Johnston, J.W. Ziller, Organometallics 24 (2005) 3916–3931, and references therein.
[5] W.J. Evans, B. Reso, J.W. Ziller, Inorg. Chem. 45 (2006) 10790–10798, and references therein.
[6] H. Reddmann, M. Karbowiak, H.-D. Amberger, J. Drożdżyński, Z. Anorg. Allg. Chem. 632 (2006) 1953–1955.

[7] H.-D. Amberger, H. Reddmann, unpublished results.
[8] M. Karbowiak, J. Drożdżyński, unpublished results.
[9] C. Görller-Walrand, K. Binnemans, Rationalization of crystal field parametrization, in: K.A. GschneidnerJr., L. Eyring (Eds.), Handbook on the Physics and Chemistry of Rare Earths, vol. 23, Elsevier, Amsterdam, 1996 (Chapter 155), and references therein.
[10] M.F. Reid, Transition intensities, in: G. Liu, B. Jacquier (Eds.), Spectroscopic Properties of Rare Earths in Optical Materials, Springer-Verlag, Berlin, 2005, p. 98 (Chapter 155), and references therein.
[11] S. Jank, H.-D. Amberger, Acta Phys. Polon. A 90 (1996) 21–32.
[12] R.J. Strittmatter, B.E. Bursten, J. Am. Chem. Soc. 113 (1991) 552–559.
[13] H. Schumann, M. Glanz, H. Hemling, F.E. Hahn, Z. Anorg. Allg. Chem. 621 (1995) 341–345.
[14] H. Schulz, H. Reddmann, H.-D. Amberger, J. Organomet. Chem. 461 (1993) 69–74, and references therein.
[15] C.K. Jørgensen, R. Pappalardo, H.H. Schmidtke, J. Chem. Phys. 39 (1963) 1422–1430.
[16] W. Urland, Chem. Phys. 14 (1976) 393–401.
[17] K.H. Johnson, F.C. Smith Jr., Phys. Rev. B 5 (1972) 831–843.
[18] H.-D. Amberger, H. Reddmann, S. Jank, M.I. Lopes, N. Marques, Eur. J. Inorg. Chem. (2004) 98–109.
[19] W.T. Carnall, H. Crosswhite, H.M. Crosswhite, Energy Level Structure and Transition Probabilities in the Spectra of the Trivalent Lanthanides in LaF_3, ANL Report, Appendix I, Table 1, 1977, unpublished.
[20] F. Auzel, O.L. Malta, J. Phys. (Paris) 44 (1983) 201–206.
[21] C. Qian, B. Wang, D. Deng, G. Wu, P. Zheng, J. Organomet. Chem. 458 (1993) 83–88.
[22] X.-F. Li, S. Eggers, J. Kopf, W. Jahn, R.D. Fischer, C. Apostolidis, B. Kanellakopulos, F. Benetollo, A. Polo, G. Bombieri, Inorg. Chim. Acta 100 (1985) 183–199.
[23] S.P. Tandon, P.C. Mehta, J. Chem. Phys. 52 (1970) 5417–5420.
[24] E.D. Brady, D. Erik, D.L. Clark, J.C. Gordon, P.J. Hay, D.W. Keogh, R. Poli, B.L. Scott, J.G. Watkin, Inorg. Chem. 42 (2003) 6682–6690.